Available online at www.sciencedirect.com
ScienceDirect
Journal of the European Ceramic Society 28 (2008) 1065–1071
www.elsevier.com/locate/jeurceramsoc

Reactive sintering of YAG-based materials using micrometer-sized powders

Laura Esposito *, Anna Luisa Costa, Valentina Medri

ISTEC CNR, Institute of Science and Technology for Ceramics, Via Granarolo 64, I-48018 Faenza, Italy

Available online 23 October 2007

Abstract

This study reports the understanding of the main features affecting the microstructure and optical properties of polycrystalline yttrium aluminum garnet (YAG) obtained by reactive sintering of commercial micrometer-sized powders. Two shaping techniques, cold isostatic pressing and slip casting, are studied and the properties of samples at the green stage related to the behaviour during vacuum sintering, to the final microstructure and the transparency.

The most promising results in terms of transparency and final density were obtained by cold isostatic pressing, whereas high green densities were obtained by slip casting, but a non-homogeneous particle packing inhibits the pore closure during sintering, thus limiting the final density and the transparency.

Keywords: Polycrystalline YAG; Shaping; Sintering; Microstructure-final; Optical properties

1. Introduction

In recent years YAG-based ceramics have been studied as solid-state laser sources in laser machines.[1–5] Compared to the more commonly used single crystals, polycrystalline ceramics can be highly doped, cheaper, faster and easier to produce.

Powders within the nanometric range are generally selected for the reactive sintering process of these materials with the purpose of improving the density and limiting the grain growth.[6–9] However, the handling and contamination control of nanometric powders are often difficult and the reliability of the process is poor.[6,10] Micrometric powders, on the other hand, if properly shaped may equally promote homogeneous particle coordination and at the same time result in formation of fine grained microstructures.[11]

Purpose of the present study is to process micrometer-sized powders through two different shaping techniques, slip casting and cold isostatic pressing, and to compare the results in terms of final microstructure and transparency after different vacuum sintering conditions.

2. Experimental

The properties of the oxide powders used for the reactive sintering process are summarized in Table 1. The powders are mixed in the stoichiometric composition of 0.8 at% Nd:YAG. The morphology of the as-received powders and after the standard ball milling treatment is shown in Fig. 1.

The weight loss and the exothermic/endothermic transformations of samples were determined by thermogravimetry (TGA) and differential thermal analyses (DTA) performed with a heating rate of 10 K/min using a simultaneous thermal analyser (STA 409, Netzsch). After thermal analyses, as well as after sintering cycles, crystalline phases were identified by X-ray diffraction analyses (Rigaku Miniflex, Cu Kα radiation).

2.1. Cold isostatic pressing (CIP)

The powders (Table 1) were ball milled for 24–96 h in ethanol using 99.9% pure Al_2O_3 milling balls, with PEG (400 or 200) as dispersant (1 wt%) and TEOS (tetraethyl orthosilicate) as sintering additive (0.5 wt%). The mixed powders were dried with Rotavapor and stored for 24 h at 70 °C for the complete removal of ethanol. The powders were then sieved through a 75 μm-mesh. Pellets with a diameter from 1 to 3 cm were obtained by axial pressing followed by cold isostatic pressing (CIP) at 250 MPa.

* Corresponding author. Tel.: +39 0546 699748; fax: +39 0546 46381.
E-mail address: laura@istec.cnr.it (L. Esposito).

0955-2219/$ – see front matter © 2007 Elsevier Ltd. All rights reserved.
doi:10.1016/j.jeurceramsoc.2007.09.006

Table 1
Properties of the powders

Material	Purity (%)	BET SSA (m^2/g)	D_{50} (μm)
Al_2O_3 Taimei	99.99	13.11	0.20
Y_2O_3 Alfa Aesar	99.999	7.56	3.91
Nd_2O_3 CRM	99.95	8.34	0.03–0.05

Al_2O_3: Taimei TM-DAR, Y_2O_3: Alfa Aesar Reacton®, Nd_2O_3: China Rare Materials (CRM) Nano-Nd_2O_3. Purity levels are manufacturer data. The BET single point method is used for the specific surface area (SSA) measurement. Particle size distribution analysis by SediGraph.

2.2. Slip casting (SC)

The slurries for the SC process were prepared in two ways[11]:

1. *SC1*: Powders directly mixed (by fast eccentric milling and/or ball milling) in water with proper type and amount of dispersant according to zeta potential measurements (Acoustoziser II, Colloidal Dynamics, USA) and sedimentation tests.
2. *SC2*: Powders previously dispersed in ethanol as described for the CIP process, dried and finally dispersed in water with a dispersant.

In both cases the slurries were ball milled for at least 24 h with 99.9% pure Al_2O_3 milling balls, with TEOS (0.5 wt%) as sintering aid and de-aired under vacuum before casting into gypsum moulds. The powder/water volume ratio of the slurry was 50/50.

2.3. Debinding cycle

The removal of organic components was performed in air with a heating rate of 50 K/h up to 500 °C and a maximum temperature of 1100 °C, i.e. in agreement to the critical temperatures steps highlighted by the TG-DTA analysis. In some cases, a maximum temperature of 1500 °C was selected.

2.4. Sintering cycles

Sintering cycles under high vacuum with Mo–W heating elements and a chamber furnace of the same material, at 1650–1750 °C for 4–6 h, were performed on selected samples. Annealing cycles in air were also performed on selected samples after vacuum sintering.

Scanning electron microscopy (SEM) (Leica Cambridge Stereoscan 360) coupled with an energy-dispersive X-ray spectrometer (EDS) was used for the microstructure characterization.

Laser transmission was measured at Vilnius University: the laser transmission measurements at 1064 nm were performed at a distance of 1–6 mm on 1 μm mirror-polished samples.

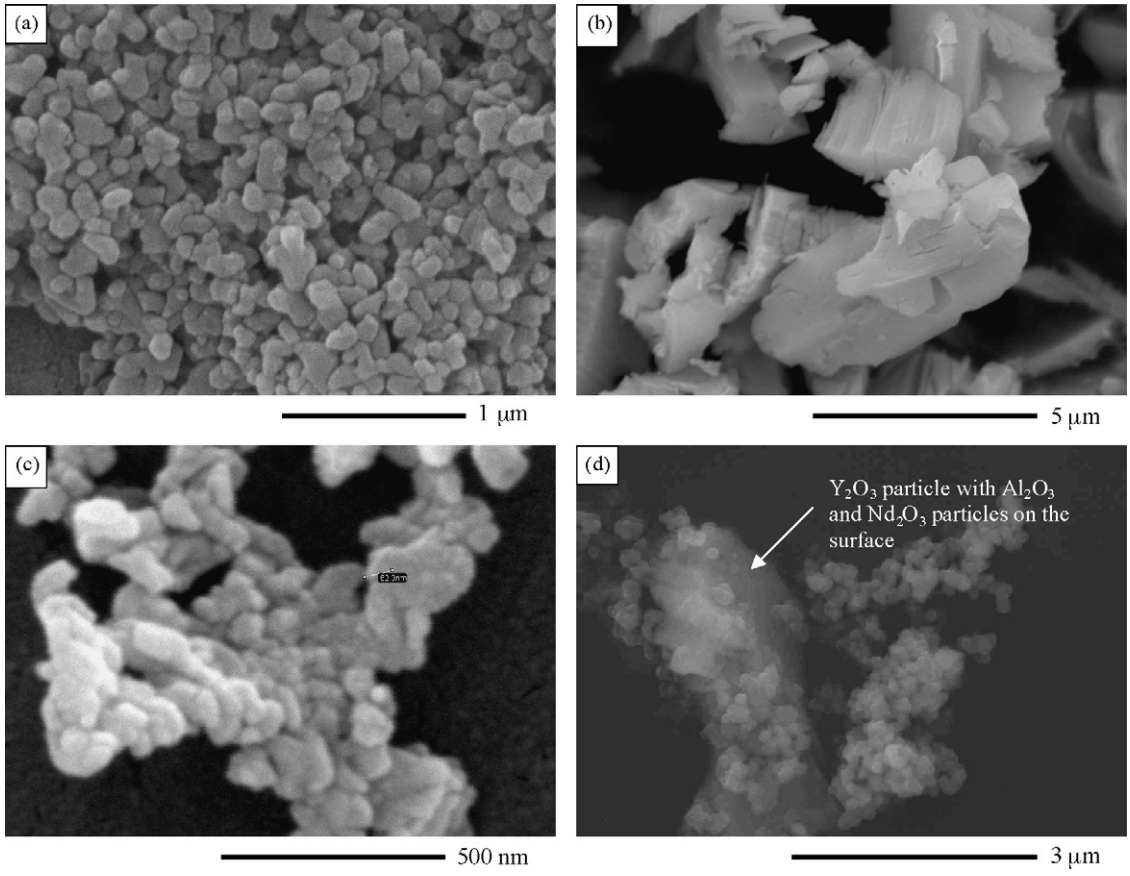

Fig. 1. Al_2O_3 Taimei TM-DAR (a), Y_2O_3 Alfa Aesar (b), Nd_2O_3 China Rare Materials (c), mixture of powders after ball milling for 48 h and drying by Rotavapor (d).

Table 2
Properties of cold isostatic pressed (CIP) and slip cast (SC) samples before (green) and after sintering in air at 1650 °C for 10 h

Sample	Linear shrinkage (%)		Density (%)	
	Green	Sintered	Green	Sintered
CIP	–	–	∼59	99.4
SC1	2.9	16.8	∼55	98.6
SC2	2.2	13.1	∼60–65	99.0

3. Results

3.1. The powders

The oxide powders selected for the reactive sintering process were all of high purity (Table 1). The alumina and yttria micrometer-sized powders have a spherical and irregular morphology, respectively (Fig. 1a and b). The relatively low SSA value exhibited by the Nd_2O_3 powder is due to the agglomerates, also shown by the SEM analysis. The nanometric nature and the agglomerates of the Nd_2O_3 powder (Fig. 1c) do not influence the forming process because the amount of this oxide in the selected Nd:YAG composition is very limited. After ball milling and drying a homogeneous mixture of the powders is obtained (Fig. 1d).

3.2. The shaping process

The relatively coarse nature of the yttria and alumina powders used for the reactive sintering process helps their handling in the course of the whole forming process. In particular, the weighting operations are easier and more precise in comparison to nanometric powders because of lower amount of adsorbed water.[12]

The CIP shaping process requires ball milling of the dispersion in ethanol in order to obtain an intimate mixing of the involved powders. No contamination from the milling media was found after ball milling treatments of up to 100 h and no additional phases formed during sintering, as explained in more detail in the following section. Contamination is minimized by slow milling, which limits the wear of the milling media and guarantees an optimal mixing among the powders.

The green density obtained by the CIP process is about 59% of the theoretical density (Table 2). This value is in line with the densities that are generally obtained by this shaping process. The use of a dispersant favours better packing of the particles by improving their mutual sliding during the CIP process, thus avoiding the formation of macroscopic pores, which could not be eliminated by sintering.

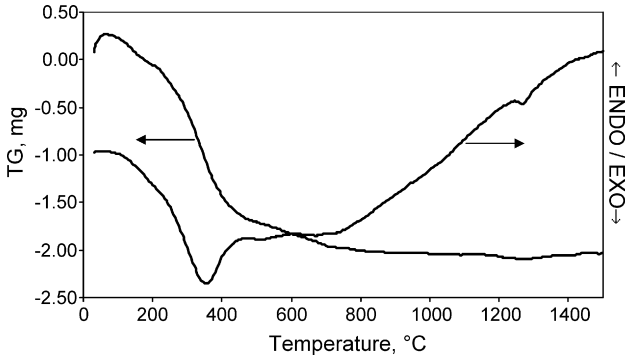

Fig. 2. TG-DTA analyses of SC2 (Table 2).

Both slurries prepared for the SC process were characterized by a high solid content (approximately 50 vol%). The green densities of the cast samples are shown in Table 2. Despite the higher shrinkage, sample SC1 exhibits a lower green and sintered density than sample SC2.

3.3. The debinding cycle

The debinding cycle is necessary for the removal of organic additives used during the shaping process. The presence of residual carbon may promote the formation of pores and the presence of reduction reactions during the vacuum sintering cycle. A fast burning out of organic compounds may in turn break the sample or lead to formation of pores. The debinding cycle must be therefore carefully designed taking into account critical temperature steps determined by the TG-DTA analyses (Fig. 2). The removal of the organic compounds occurs for the most part in the temperature range between 100 and 500 °C, as shown by the exothermic peak of the DTA curve. The increase of the DTA curve observed above 800 °C does not represent any phase reaction in the sample and is caused by an instrument drift. The exothermic peak observed at 1270 °C is the result of the reaction between the oxides, which results in the formation of a solid solution containing the $Y_4Al_2O_9$ (YAM) and/or $YAlO_3$ (YAP) phases[5]. Around 1450 °C $Y_3Al_5O_{12}$ (YAG) is formed,[5] as confirmed by the XRD spectra carried out on the residual powders after the TG-DTA analysis up to 1500 °C. No peak is revealed in the DTA curve because of the fast heating rate (10 °C/min) adopted during the analysis. On the basis of these results, the standard binder removal cycle used in the present study was characterized by a heating rate of 50 K/h up to 500 °C and a

Table 3
Final relative density and grain size [μm] of CIP, SC1 and SC2 samples (Table 2) after different vacuum sintering and annealing cycles

Sample	1650 × 6	1650 × 6 + A.A.	1700 × 4	1750 × 4	1750 × 4 + A.A.
CIP	100 [3]	99.93 [4]	99.98 [6]	100 [6[a]]	100
SC1	98.5 [1]	99.50 [3]	99.00 [2]	–	–
SC2	–	–	99.80 [2.5]	100 [10[b]]	100

[a] Fifteen micrometer if debinded at 1500 °C × 2 h.
[b] Five micrometer if debinded at 1500 °C × 2 h.

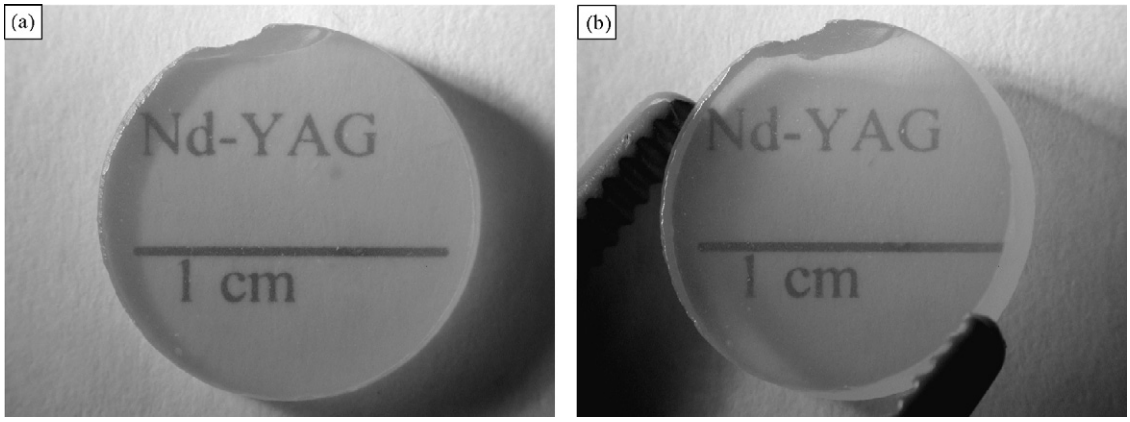

Fig. 3. (a) Optical pictures of the CIP sample debinded at 1500 °C and sintered at 1750 °C for 4 h. Picture (b) shows the tilted sample not in direct contact with the surface.

maximum temperature of 1100 °C with a soaking time of 2 h. Under these conditions, all the organics were fully eliminated whereas no transformation reactions could take place. In addition, in some cases, the debinding cycle is performed at 1500 °C in order to study the microstructure evolution if the transformation into YAG has already occurred before the vacuum sintering cycle.

3.4. The vacuum sintering and annealing cycles

The selected sintering temperature range was 1650–1750 °C with the soaking time of 4–6 h. As revealed by XRD analyses, the only crystalline phase was pure Nd:YAG phase in all the sintered samples. Fully dense samples were obtained from CIP and SC2 samples (Table 3). CIP samples sinter to full density already from 1650 °C whereas the temperature of 1750 °C is necessary to obtain fully dense SC2 samples. SC1 samples do not sinter to full density under the sintering conditions applied. According to Krell et al.,[6] SC samples can be defined as translucent, whereas CIP samples exhibit a limited transparency. The CIP sample debinded at 1500 °C and sintered at 1750 °C for 4 h, exhibits the higher transparency among all samples (Fig. 3). The transmission value is however relatively small if compared with the value of a commercial Nd:YAG material used as reference for the transmission measurements (Table 4). Conversely, the SC1 sample debinded at 1500 °C instead of 1100 °C exhibits a larger grain size after densification.

The post-annealing cycle in air at 1650 °C for 20 h of samples exhibiting a density of at least 96% of the theoretical one (i.e. with a closed porosity), improves the density and translucency only in the case of SC1 sample vacuum sintered at 1650 °C. The CIP sample vacuum sintered at the same temperature up to full density de-sinters slightly after the annealing cycle and becomes less transparent. No density or translucency change was observed after annealing in the case of SC2 and CIP samples vacuum sintered up to full density at 1750 °C.

The microstructures of CIP and SC1 samples debinded in air at 1100 °C and sintered under vacuum at 1650, 1700 °C and at 1650 °C followed by annealing at 1650 °C for 10 h are shown in Fig. 4. Full density is reached only with CIP at 1650 °C and the grain size increases with temperature. SC1 samples exhibit smaller grains than CIP. The best SC1 sample in terms of density and amount of residual pores is the sample post-annealed in air; however, the laser transmission did not improve despite only limited grain growth. The presence of pores is possible even in samples which were found to be fully dense by the Archimedes method because the accuracy of the method is not sufficient for densities higher than 99.9%.

Fig. 5 shows the microstructures of CIP and SC2 samples debinded at 1100 and 1500 °C and vacuum sintered at 1750 °C. The debinding temperature affects the final grain size, which increases with CIP when the debinding is conducted at 1500 °C instead of 1100 °C, whereas the opposite occurs for SC2. During the debinding cycle at 1500 °C the starting oxides react and form YAG,[5] as confirmed by XRD analyses after TG-DTA up to 1500 °C.

4. Discussion

The CIP samples are generally characterized by smaller pores and by a lower amount of residual porosity as well as a microstructure with larger grains compared to SC samples

Table 4
Laser transmission of samples @ 1064 nm wavelength

Sample	Transmission (%)						Average (%)
	1 mm	2 mm	3 mm	4 mm	5 mm	6 mm	
CIP	38.9	36.3	36.3	38.1	38.1	37.2	37.4
Commercial Nd:YAG	84.5	84.3	84.3	84.3	83.0	83.4	84.4

Measurements carried out at the Vilnius University (Prof. Valdas Sirutkaitis). The CIP sample is debinded in air at 1100 °C for 2 h before vacuum sintering at 1750 °C for 4 h. The commercial Nd:YAG material used as the reference is produced by Konoshima Chemical Co. Ltd. and contains 1.1 at% of neodymium.

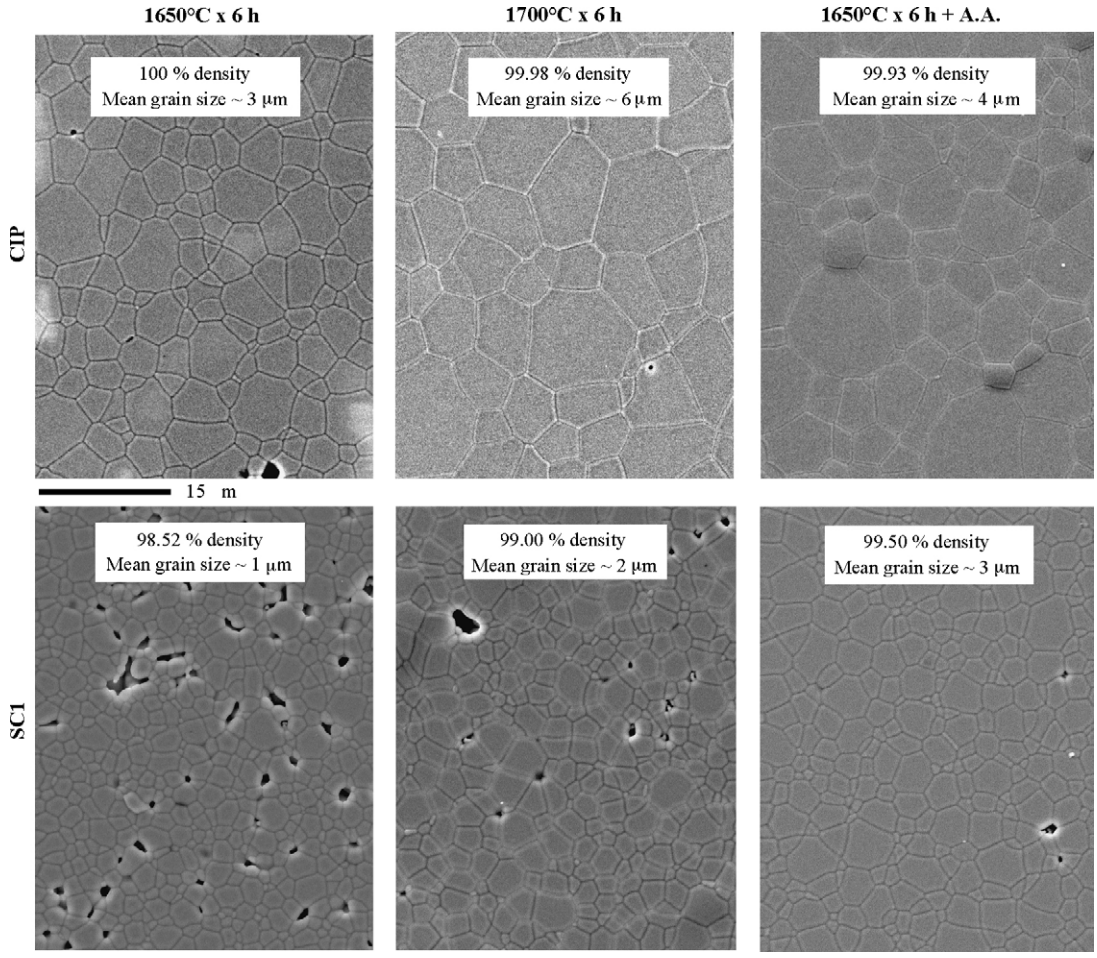

Fig. 4. Microstructure of CIP and SC1 samples after different vacuum sintering and air annealing cycles. Debonding conducted at 1100 °C × 2 h with a slow heating rate.

(Fig. 4). This feature is a consequence of the slower densification rate of SC samples, which consequently inhibits the grain growth. An example in this sense is represented by the samples debinded at 1100 and 1500 °C (Fig. 5). The SC sample exhibited larger grains than CIP samples if debinded at 1100 °C but smaller if debinded at 1500 °C. The debinding cycle at high temperature of the less homogeneous SC sample probably promoted its partial densification and formation of entrapped pores which, during the vacuum sintering, inhibit the complete densification.[13–15] On the contrary, CIP samples are characterized by a more homogeneous particle packing and consequently the debinding at 1500 °C enhance the grain growth. The residual pores are also responsible for lower transparency observed in the SC samples. The SC2 sample debinded at 1100 °C and sintered at 1750 °C is in fact only slightly transparent, whereas the CIP sample sintered under the same conditions exhibited a higher transparency (Fig. 3).

Residual pores affect the sintering behaviour of the samples even during the annealing cycle in air. After the vacuum sintering at 1650 °C, samples exhibit a closed porosity with pores containing no air. The final densification stage is mainly kinetically controlled[13,14,16] and depends on the size and amount of pores as well as on the grain size but no influence may be expected from the furnace atmosphere. A long air annealing cycle at a temperature lower than the previous vacuum sintering cycle has the advantage of promoting the closure of the residual pores with a limited grain growth. In addition, an annealing cycle in air or even under O_2-rich atmosphere, may promote the decolouring of the sample through the oxidation of phases which partially reduced during vacuum sintering.[3,5] Indeed, the pore closure with a limited grain growth and a density increase, is observed in case of SC2 sample (Fig. 4). The CIP sample which was fully dense after the vacuum sintering cycle, underwent a partial de-sintering together with limited grain growth.

A partial depletion of TEOS, used as sintering additive, during the casting operations can be hypothesized in SC1 samples which do not sinter up to full density under any of the tested sintering conditions. This effect was not observed in case of SC2 samples because the double mixing treatment, first in ethanol and then in water, promotes the hydrolysis of TEOS and its homogeneous distribution onto the oxide particles surface. The direct mixing in water, on the contrary, inhibits the TEOS hydrolysis, which consequently may be drawn up into the gypsum mould during casting.

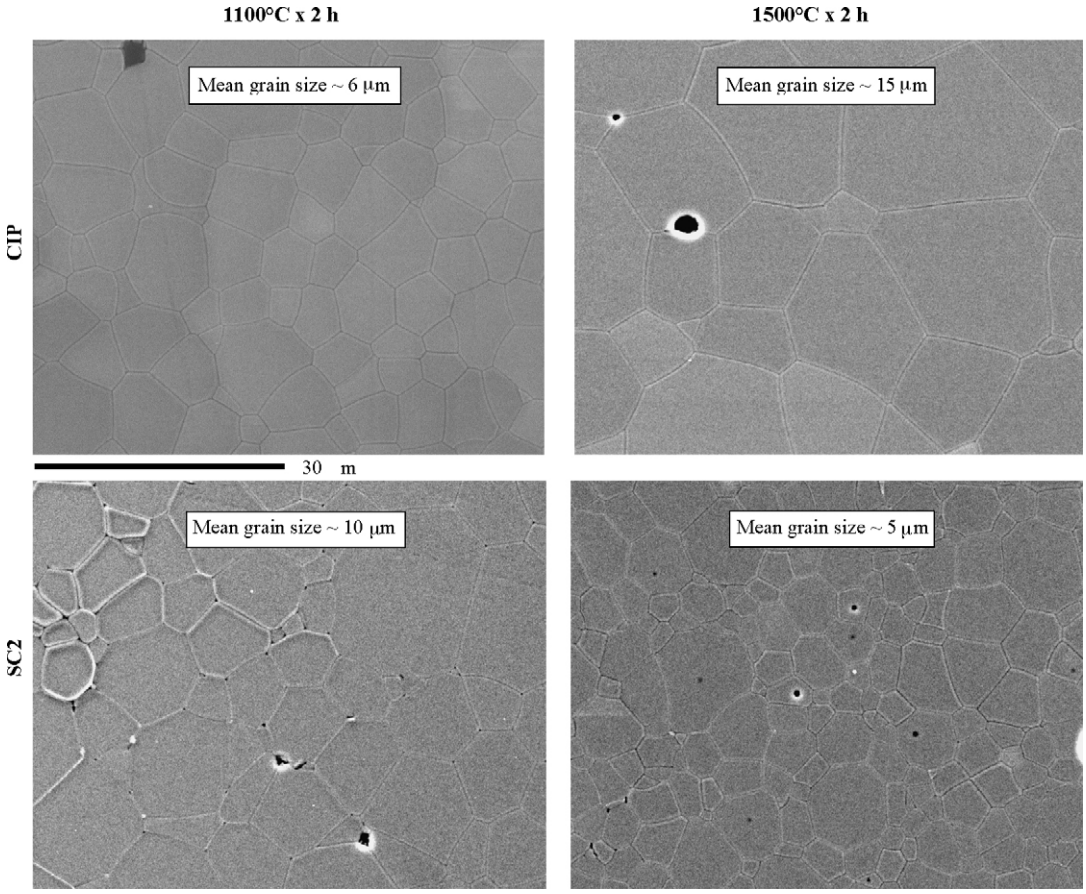

Fig. 5. Microstructure of CIP and SC2 double-mixed samples after vacuum sintering at 1750 °C × 4 h after different debinding cycles.

5. Conclusions

Micrometer-sized powders are possible candidates for replacement of nanometric ones for the production of transparent YAG-based materials. The most promising results were obtained with CIP samples debinded at 1500 °C and vacuum sintered at 1750 °C. High green densities were obtained by slip casting, but a non-homogeneous particle packing inhibits the pore closure during sintering, thus limiting the final density and the transparency. Pore closure is a key feature of transparent ceramics. Post-annealing cycles are effective in improving the density by closing the residual pores and limiting the grain growth, but samples must exhibit a small, limited porosity and grain size. Attention must be paid to careful control of the shaping process since pore-free, transparent ceramics can be obtained only with a highly homogeneous particle packing.

Acknowledgements

This work was conducted in the frame of the European CRAFT Project NOVIGLAS Contract No. COOP-CT-2004-512318.

The authors wish to thank Dr. Eckhard Sonntag, Broell GmbH & Co./Austria, for the useful suggestions and fruitful discussions.

References

1. Ikesue, A., Aung, Y. L. and Synthesis, Performance of advanced ceramic lasers. *J. Am. Ceram. Soc.*, 2006, **89**(6), 1936–1944.
2. Yagi, H., Transparent YAG ceramics. *Bull. Am. Ceram. Soc.*, 2005, **84**(5), 9.
3. Takagimi, Y. and Hideki, Y., Rare earth garnet sintered compact. US Patent 2005/0,215,419 A1 (September 29, 2005).
4. Lee, H. D., Mah, T., Parthasarathy, T. A. and Keller, K. A., YAG lasing systems and methods. US Patent 2005/0,281,302 A1 (December 22, 2005).
5. Lee, S.-H., Kochawattana, S. and Messing, G., Solid-state reactive sintering of transparent polycrystalline Nd:YAG ceramics. *J. Am. Ceram. Soc.*, 2006, **89**(6), 1945–1950.
6. Krell, A., Hutzler, T. and Klimke, J., Transparent ceramics for structural applications. Part 1. Physics of light transmission and technological consequences Ceramic Forum International Ber. *DKG*, 2007, **84**, 4.
7. Rabinovitch, Y., Tétard, D., Faucher, M. D. and Pham-Thi, M., Transparent polycrystalline neodymium doped YAG: synthesis parameters laser efficiency. *Opt. Mater.*, 2003, **24**, 345–351.
8. Matsushita, N., Tsuchiya, N., Natatsuka, K. and Yanagitani, T., Precipitation and calcination process for yttrium aluminum garnet precursors synthesized by the urea method. *J. Am. Ceram. Soc.*, 1999, **82**(8), 1977–1984.
9. Feng, T., Shi, J. and Jiang, D., Preparation and optical properties of transparent Eu^{3+}:$Y_3Al_{5(1-x)}Sc_{5x}O_{12}$ ceramics. *J. Am. Ceram. Soc.*, 2006, **89**(5), 1590–1593.
10. Costa, A. L., Esposito, L., Medri, V. and Bellosi, A., Synthesis of Nd-YAG material by citrate nitrate sol-gel combustion route. *Adv. Eng. Mater.*, 2007, **9**, 307–312.

11. Esposito, L. and Piancastelli, A., Role of powder properties and shaping techniques on the formation of pore-free YAG materials. *Proceeding of the 10th international conference and exhibition of the European Ceramic Society*, June 17–21, 2007, Berlin, submitted for publication.
12. Esposito, L. and Medri, V., Properties of YAG based materials obtained by reactive sintering of nanometric powders, in preparation.
13. Slamovich, E. B. and Lange, F. F., Densification of large pores. I. Experiments. *J. Am. Ceram. Soc.*, 1992, **75**(9), 2498–2508.
14. Lee, S.-H. and Yang, J.-K., Elimination of large artificial pores during the hot isostatic pressing of presintered alumina. *J. Am. Ceram. Soc.*, 1993, **75**(4), 880–884.
15. Ikesue, A., Yoshida, K., Yamamoto, T. and Yamaga, I., Optical scattering centers in polycrystalline Nd:YAG laser. *J. Am. Ceram. Soc.*, 1997, **80**(6), 1517–1522.
16. Krell, A. and Hutzler, T., Transparent polycrystalline sintered ceramic of cubic crystal structure. US Patent US 2005/0,164,867 A1 (July 28, 2005).